Journal of the Korean Physical Society, Vol. 55, No. 2, August 2009, pp. 558∼561

Microscopic Characterization of Silicon Nanocrystals Formed by *In-situ* Annealing

Sung Won Hwang, Dong Hee Shin, Seung Hui Hong and Suk-Ho Choi*
Department of Applied Physics, College of Applied Science, Kyung Hee University, Yongin 446-701

(Received 11 May 2009)

Scanning tunneling microscopy (STM) and atomic force microscopy were used for characterizing Si nanocrystals (NCs) embedded in SiO_2. The Si NCs were formed by *in-situ* annealing of Si-rich oxide (SiO_x) films grown by ion beam sputtering. The thickness of the SiO_x layers was 200 nm, and the annealing was done at 1165 °C for 3 min. The sizes and the densities of the Si NCs were estimated as $4 \sim 2.5$ nm and $6.2 \times 10^{11} \sim 3.4 \times 10^{12}$ cm^{-2}, respectively, for $x = 1.2$ to 1.8, almost consistent with the high-resolution transmission electron microscopy (HRTEM) results. The photoluminescence peak of the Si NCs blueshifts from 1.44 to 1.63 eV as x increases from 1.0 to 1.8, as expected by the quantum confinement effect based the NC-size variation measured by using STM and HRTEM. These results demonstrate that STM is an accurate tool for characterizing the distributions of sizes and densities for Si NCs.

PACS numbers: 61.46.Hk, 68.37.Ef, 68.37.Ps, 78.55.Ap
Keywords: Silicon nanocrystals, Scanning tunneling microscopy, Atomic force microscopy, Photoluminescence

I. INTRODUCTION

Nanosized semiconductor particles have been investigated extensively during the past several years because they show novel properties different from those of their bulk counterparts. When the dimension of the nanoparticles is smaller than the corresponding exciton Bohr radius, they exhibit a number of striking behaviors, such as quantum confinement (QC) and optical nonlinearities. Especially, Si nanocrystals (NCs) have received enormous attention and have been studied intensively in view of their potential applications in optoelectronics devices because a strong light emission was found in Si NCs at room temperature [1, 2]. As reported previously [3,4], Si NCs formed within host materials such as SiO_2 have broad distributions of sizes and orientations, and many oxygen-related defect centers exist at the Si NCs/SiO_2 interfaces. This explains why the photoluminescence (PL) emission spectra of such materials have typically broad bands [5, 6]. The Si=O or Si-O bonds are known to exist at the Si NCs/SiO_2 interfaces, which significantly reduce the effective optical band gap by creating localized states and pinning the band gap of Si NCs, resulting in a PL peak shift smaller than expected from quantum confinement effect (QCE) [7–9]. Therefore, it is important to well characterize and control the Si NCs/SiO_2 interfaces. On the other hand, it is also essential to control the size and the density of Si NCs as accurately as possible for their application to Si-NC floating gate memories. Transmission electron microscopy (TEM) is the most-widely used tool to characterize the size and the density of Si NCs [10–12], but it is always a difficult job to make specimens for TEM. Recently, scanning tunneling microscopy (STM) was employed to characterize Si NCs and was shown to be promising as a tool for the quantitative analysis of Si NCs [13,14].

In this paper, we first introduce in-situ annealing for the formation of Si NCs, followed by a structural analysis by using ultra-high-vacuum (UHV) STM. We also characterize Si NCs by using high-resolution TEM (HRTEM), tapping-mode atomic force microscopy (AFM), and PL. We compare the results with those obtained by using STM.

II. EXPERIMENT

SiO_x films of 200 nm thickness were grown on n-type (100) Si wafers at room temperature by using an Ar^+ beam with an ion energy of 750 eV and a Si target under an oxygen atmosphere in a reactive ion beam sputtering deposition (IBSD) system with a Kaufman-type dc ion gun. The relative film thickness was controlled by using the growth rate calibrated by TEM measurements of thin films grown within a given time. The deposition chamber was evacuated to a pressure of 5.0×10^{-9} Torr before introducing argon gas into the system. The details of the system are described elsewhere [15]. The stoichiometry

*Corresponding Author: sukho@khu.ac.kr

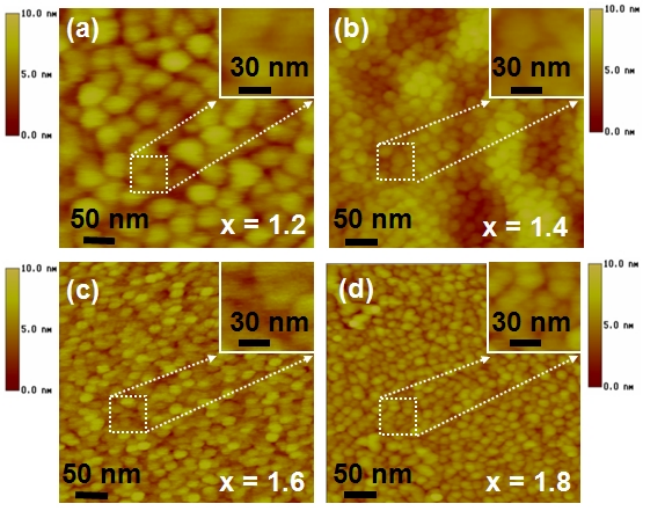

Fig. 1. AFM topography images (400 nm × 400 nm) of the Si NCs formed by annealing SiO_x films with (a) $x = 1.2$, (b) $x = 1.4$, (c) $x = 1.6$, and (d) $x = 1.8$. The insets show higher magnification images taken at the region of the marked white box. The vertical scale bar on each figure indicates the dimension in the direction of the depth from the surface.

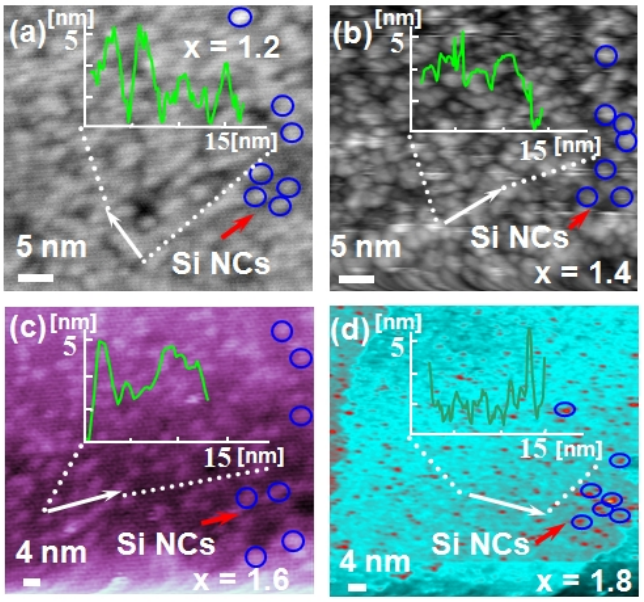

Fig. 2. STM topography images of Si NCs for (a) $x = 1.2$, (b) $x = 1.4$, (c) $x = 1.6$, and (d) $x = 1.8$. The inset shows the line profile scanned along the direction marked by the white arrow. Blue circles are drawn to indicate Si NCs as a guide for the eye.

of the SiO_x films could be analyzed and controlled by using in situ X-ray photoelectron spectroscopy (XPS) with the Al Kα line at 1486.6 eV. The oxygen fraction of the samples was controlled by changing the oxygen partial pressure. The stoichiometry (x) was determined from the relative sensitivity factors (RSFs) of the Si 2p and the O 1s peaks, which were calculated by using an in-situ XPS analysis of stoichiometric SiO_2 thin films.

After the substrates had been etched in a buffered hydrofluoric solution for several min, they were loaded into an ultrahigh vacuum chamber equipped for STM. The vacuum chamber was kept at 1×10^{-10} Torr to avoid further oxidation of Si. The in-situ annealing of the SiO_x films was performed at 1165 °C for 3 min to form Si NCs. STM operations were done at room temperature using a tungsten scanning tip in the constant current mode under a filled state with a bias of –3.5 V and a tunneling current of 1.5 nA. The tips used for STM were obtained by electrochemical etching of a polycrystalline tungsten wire in a solution of 2-M potassium hydroxide (KOH), followed by in-situ electron bombardment, allowing us to reproducibly get high-quality apices suitable for imaging corrugated surfaces. The lateral size of Si NCs was estimated by measuring the full width at half maximum height of the STM data. The topography of the Si NCs and their surface evolution were also studied ex situ by using tapping-mode AFM. PL spectra were measured at room temperature by using the 488 nm line of an Ar^+ laser as the excitation source. Emitted light was collected by using a lens and was analyzed using a grating monochromator and a PM tube. Standard lock-in detection techniques were used to maximize the signal-to-noise ratio. The laser beam's diameter was about 300 μm, and its power was about 50 mW.

III. RESULTS AND DISCUSSION

Figure 1 shows tapping-mode AFM images of the Si NCs formed by annealing the SiO_x films with different x values of $1.2 \sim 1.8$. For better images, the SiO_2 layers on the sample surface were etched in a buffered hydrofluoric-acid solution. The insets show higher magnification images taken at the region of the marked white box. The NCs are roughly spherical and uniform in size with a root mean square (RMS) size of 0.842 nm. The NC densities are estimated as $4.6 \times 10^8 \sim 8.1 \times 10^{10}$ cm^{-2} for x from 1.2 to 1.8. These are underestimated values because the particles seen in the images are in fact clusters of NCs, resulting from the much larger size of the tip compared to that of NCs [16]. These results suggest that the formation of Si NCs within a SiO_2 layer can be identified qualitatively by using AFM.

Figure 2 shows filled-state STM images of the Si NCs formed by in-situ annealing of the SiO_x films with different x values of $1.2 \sim 1.8$. The insets show the line profile scanned along the marked white line of 15 nm. Before STM operations, the samples were etched with buffered hydrofluoric acid to remove SiO_2, leaving the Si NCs to be exposed on the surface. The brightly-protruding islands in the STM images indicate the Si NCs, whose existence is also confirmed by an analysis of the height distribution of the NC protrusions through a line-profile

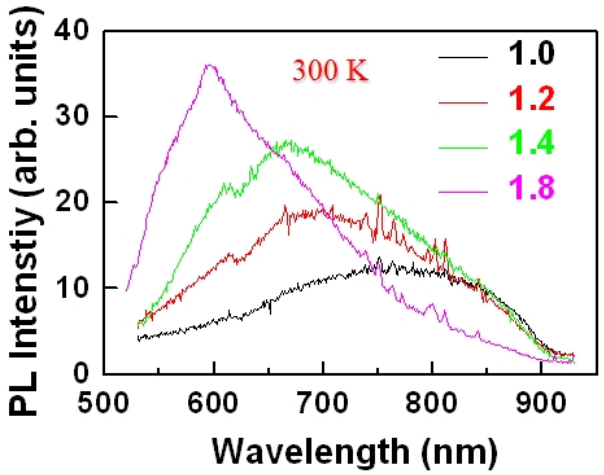

Fig. 3. Room-temperature PL spectra of Si NCs for various x values.

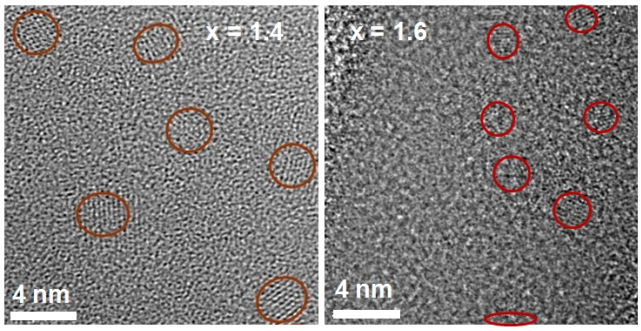

Fig. 4. HRTEM images of Si NCs for $x = 1.4$ and 1.6.

scan. The interconnected Si NCs have a RMS roughness of 0.29 nm. The size of NCs is defined as the peak-to-peak width in the line profile mainly determined by their spherical shape. The size of the NCs is quite uniform in the range of the scan and is estimated as 4 $\sim$ 2.5 nm for various x values. A statistical analysis carried out on about 167 islands gives an aspect ratio of 0.35 $\pm$ 0.06. The shape of the STM tip could influence the size of the protruding objects. Since this tip convolution effect occurs even for a sharp STM tip, the line profile of an individual NC cannot be used to obtain an accurate height or aspect ratio. The density of NCs on a fully etched sample is measured to be around 6.2 $\times$ 10^{11} $\sim$ 3.4 $\times$ 10^{12} cm^{-2} for various x values. These values are still lower bounds, considering the loss of NCs during the etching process. The shape of the Si NCs is roughly spherical, in good agreement with the HRTEM and AFM observations.

Figure 3 shows the room-temperature PL spectra of SiO_x films with different x values after annealing. The Si NCs at $x = 1.0$ shows a broad PL spectrum centered at around 1.57 eV, in agreement with the estimated recombination energy for quantum-confined excitons in $\sim$3.5-nm diameter Si NCs [4]. The width of the emission band

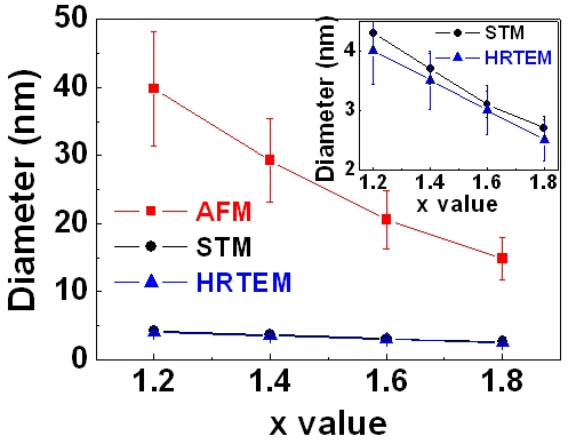

Fig. 5. Si NC diameter-versus-x plots extracted from AFM, STM, and TEM results. The inset shows the magnified plots of the STM and the TEM results.

is attributed to the wide distribution in NC sizes [3–5]. When x varies from 1.0 to 1.8, the PL band blueshifts from 790 nm (1.57 eV) to 597 nm (2.08 eV), consistent with the quantum confinement effect due to the size reduction of Si NCs by the increased oxygen fraction [4, 17,18]. The total shift of the PL peak is about 0.51 eV, which is larger than the previously-reported values [19, 20], possibly resulting from a reduction in the interface states, such as Si=O or Si-O bonds, around Si NCs [7,9] by in-situ UHV annealing.

Figure 4 shows the dark-field plane-view HRTEM images of the SiO_x films with $x = 1.4$ and 1.6 after annealing. The Si NCs, as recognized from the lattice fringes, are randomly dispersed in the SiO_2 matrix. The mean diameters of the Si NCs at $x = 1.4$ and 1.6 are 3.5 $\pm$ 0.8 nm and 3.0 $\pm$ 0.6 nm, respectively, in good agreement with the results given by the STM images. The NC densities are estimated to be 1.4 $\times$ 10^{12} and 3.1 $\times$ 10^{12} cm^{-2} for $x = 1.4$ and 1.6, respectively.

Figure 5 compares the average diameters of Si NCs analysed by using AFM, STM, and HRTEM. The inset shows magnified plots of the STM and the HRTEM results. All plots show decreasing behaviors of the NC size with increasing x, but the diameters obtained by using AFM are much larger than those obtained by STM and TEM. Both STM and TEM data are almost identical. These results suggest that the AFM results do not reflect the real sizes of the Si NC. The values of the error bars are approximately 21, 7, and 14% for AFM, STM, and HRTEM, respectively, indicating that STM is the most accurate tool for a size analysis of Si NCs.

IV. CONCLUSION

SiO_x films were grown by IBSD under varying conditions of oxygen content and were subsequently annealed

in situ in a STM system at 1165 °C for 3 min, which led to the formation of Si NCs within the SiO_2. The Si NCs were characterized by using STM, AFM, HRTEM, and PL measurements. The sizes and the densities of Si NCs, extracted from the STM results, were estimated as $4 \sim 2.5$ nm and $6.2 \times 10^{11} \sim 3.4 \times 10^{12}$ cm^{-2}, respectively, for x from 1.2 to 1.8. Their values were almost consistent with those from HRTEM. The PL peak of the Si NCs blueshifted from 1.44 to 1.63 eV as x increased from 1.0 to 1.8, as expected from the QCE based on the NC-size variation analyzed by using STM and HRTEM. These results suggest that STM is a promising tool for structural characterizations of the sizes and the densities of Si NCs within SiO_2.

ACKNOWLEDGMENTS

This work was supported by New & Renewable Energy R&D program (2008-N-PV08-J-02-0-000) under the Ministry of Knowledge Economy.

REFERENCES

[1] A. Irrera, F. Iacona, I. Crupi, C. D. Presti, G. Franzò, C. Bongiorno, D. Sanfilippo, G. D. Stefano, A. Piana, P. G. Fallica, A. Canino and F. Priolo, Nanotechnology **17**, 1428 (2006).

[2] L. D. Negro, J. H. Yi, J. Michel, L. C. Kimerling, T.-W. Chang, V. Sukhovatkin and E. H. Sargent, Appl. Phys. Lett. **88**, 233109 (2006).

[3] O. Jambois, H. Rinnert, X. Decaux and M. Vergnat, J. Appl. Phys. **98** 046105 (2005).

[4] M. Zacharias, J. Heitmann, R. Schoiz, U. Kahler, M. Schmidt and J. Blasing, Appl. Phys. Lett. **80**, 661 (2002).

[5] L. Patrone, D. Nelson, V. I. Safarov, W. Marine and S. Giorgio, J. Appl. Phys. **87**, 3829 (2000).

[6] J. B. Khurgin, E. W. Forsythe, G. S. Tompa and B. A. Khan, Appl. Phys. Lett. **69**, 1241 (1996).

[7] X. X. Wang, J. G. Zhang, L. Ding, B. W. Cheng, W. K. Ge, J. Z. Yu and Q. M. Wang, Phys. Rev. B **72**, 195313 (2005).

[8] Z. Zhou, L. Brus and R. Friesner, Nano Lett. **3**, 163 (2003).

[9] M. V. Wolkin, J. Jorne, P. M. Fauchet, G. Allan and C. Delerue, Phys. Rev. Lett. **82**, 197 (1999).

[10] B. Garrido Fernandez, M. López, C. García, A. Pérez-Rodríguez, J. R. Morante, C. Bonafos, M. Carrada and A. Claverie, J. Appl. Phys. **91**, 798 (2002).

[11] S. Tiwari, J. A. Wahl, H. Silva, F. Rana and J. J. Welser, Appl. Phys. A: Mater. Sci. Process. **71**, 403 (2000).

[12] M. L. Ostraat, J. W. De Blauwe, M. L. Green, L. D. Bell, M. L. Brongersma, J. Casperson, R. C. Flagan and H. A. Atwater, Appl. Phys. Lett. **79**, 433 (2001).

[13] T. Baron, P. Gentile, N. Magnea and P. Mur, Appl. Phys. Lett. **79**, 1175 (2001).

[14] E. Nogales, B. Méndez, J. Piqueras and R. Plugaru, Nanotechnology **14**, 65 (2003).

[15] S. H. Hong, S. Kim, SH. Choi, K. J. Lee, H. Lee, K. J. Kim and D. W. Moon, J. Korean Phys. Soc. **45**, 116 (2004).

[16] K. C. Grabar, K. R. Brown, C. D. Keating, S. J. Stranick, S. Tang and M. J. Natan, Anal. Chem. **69**, 471 (1997).

[17] V. Vinciguerra, G. Franzo, F. Priolo, F. Iacona and C. Spinella, J. Appl. Phys. **87**, 8165 (2000).

[18] B. V. Kamenev and A. G. Nassiopoulou, J. Appl. Phys. **90**, 5735 (2001).

[19] M. C. Kim, Y. M. Park, S.-H. Choi and K. J. Kim, J. Korean Phys. Soc. **50**, 1760 (2007).

[20] S. Kim and S.-H. Choi, J. Korean Phys. Soc. **52**, 462 (2008).